Measurement of tau filament fragmentation provides insights into prion-like spreading

Supporting Information

Table of contents

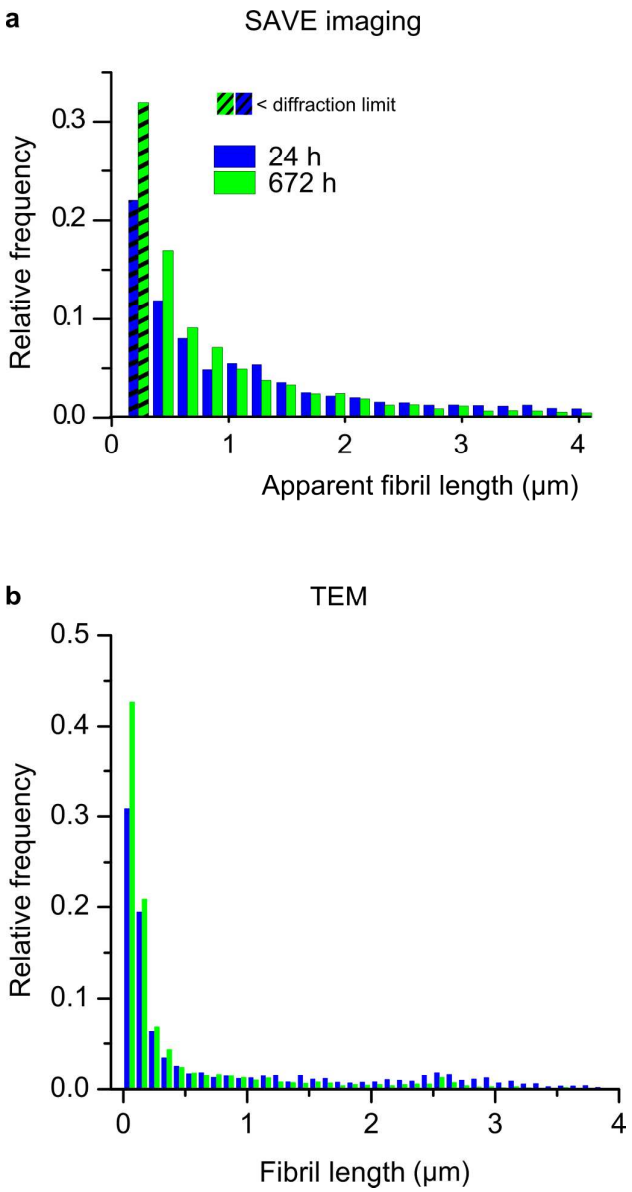

Supporting Figure 1 Fibril length distribution of P301S tau aggregates

a) Apparent fibril length distribution of P301S tau after 1 day (blue) and 26 days (green), derived from TIRF images (N=3).b) Fibril length distribution of P301S tau from electron micrographs (N=3).

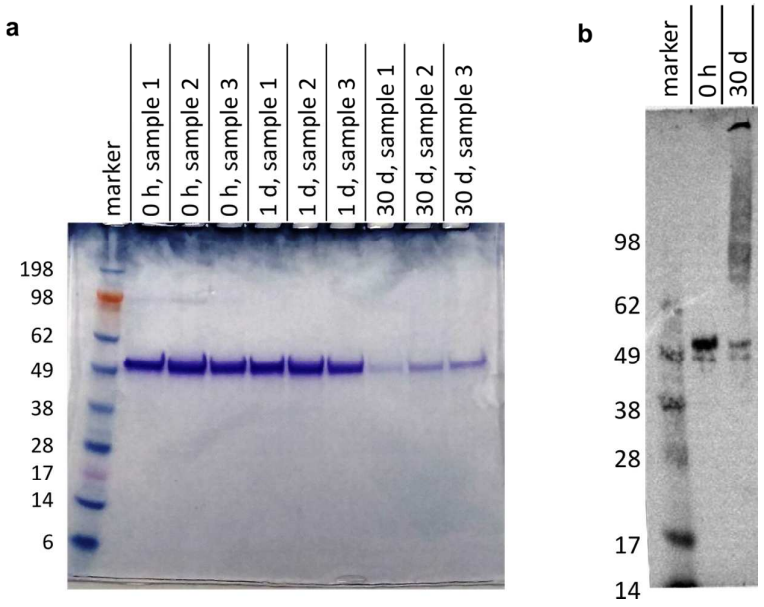

Supporting Figure 2 No signs of proteolysis during aggregation

To test for proteolytic degradation of tau, SDS-PAGE analysis was performed on aliquots from P301S tau samples during aggregation.
a) Coomassie stained gel of P301S tau samples after 0 h, 1 day and 30 days of aggregation. No degradation products are visible.
b) Western blot (HT7, anti-total tau) of P301S tau sample after 0 h and 30 days of aggregation. The sample aggregated for 30 days shows a band with tau immunoreactivity at the top of the gel, suggesting that the majority of the protein did not enter the gel.

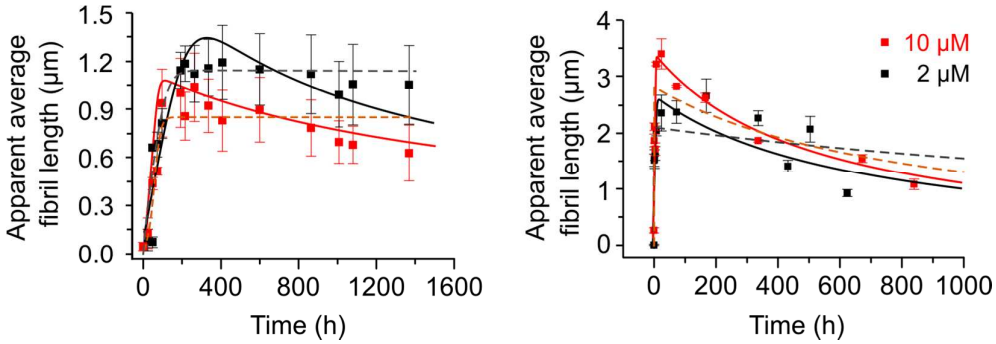

Supporting Figure 3 Misfits to a model which includes secondary nucleation

The apparent average length of WT tau (left) and P301S tau fibrils (right) as a function of time. N=3 (3 different batches of protein, each in triplicates); Error bars: s.e.m. To test if fragmentation or secondary nucleation dominate the late stages of tau aggregation, separate fits were produced for each model. Solid lines: fit to fragmentation model. Dotted lines: Misfit to secondary nucleation and ripening model (see supporting Text 1).

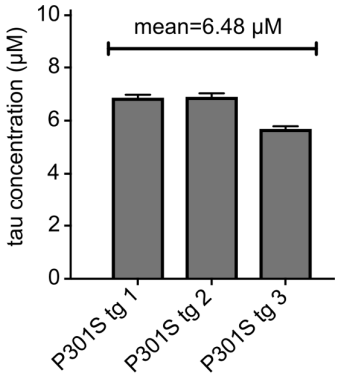

Supporting Figure 4 Concentration of P301S tau in P301S Tg mouse brains

The concentration of human tau in whole brains of three human P301S tau transgenic mice was measured by sandwich ELISA. Data represents mean of two measurements.

Spreading efficiency (%)	Number of fibrils N needed for spreading to occur	Doubling rounds per cycle	Hypothetical spreading time (years)	
			wt	P301S
100	2	1	4	0.5
10	11	3	13	1.8
1	101	7	26	3.4
0.1	1001	10	38	5.1
0.01	10001	13	51	6.7
0.001	100001	17	64	8.4
0.0001	1000001	20	77	10.1

Supporting Table 1 Hypothetical tau spreading time at different spreading efficiencies

To calculate the hypothetical spreading time (time for each brain cell to have one tau aggregate), first the number of fibrils needed for spreading to occur at a given efficiency was calculated (N=1+(100/spreading efficiency)), e.g. at a spreading efficiency of 1%, 101 fibrils have to be formed for one to seed a neighbouring cell. This will add seven extra rounds of doubling ($\log_2 N$) to each amplification cycle. The hypothetical spreading time t is therefore t=(doubling rounds per cycle)*t_2 with t_2 being the doubling time of wild-type (wt) or P301S tau (38 days or 5 days respectively). Therefore, at 1% spreading efficiency the spreading time for wild-type tau aggregates would be 26 years and for P301S tau 3.4 years.

Protein	Buffer conditions	Stirring mode	Temp.	Reference
murine PrP	50 mM Na phosphate, pH 7.0	200 rpm, shaking	37° C	(1)
α-synuclein	PBS + 0.01% NaN_3, pH 7.4	200 rpm, shaking	37° C	(1)
wild-type tau (0N4R)	SSPE + 0.02% NaN_3, pH 8.0	none	37° C	this study
P301S tau (0N4R)	SSPE + 0.02% NaN_3, pH 8.0	none	37° C	this study

Supporting Table 2 Experimental conditions for mPrP, α-synuclein and tau aggregation

Experimental conditions under which elongation and fragmentation rates shown in Figure 4 were determined.

Supporting Text 1: Determination of average fibril length using reversible polymerization model without fragmentation

When aggregates are formed through primary and secondary nucleation pathways and grow by reversible polymerization (elongation and monomer dissociation), the system kinetics are described by the following kinetic equations:

$$\frac{dP(t)}{dt} = k_n m(t)^{n_c} + k_2 m(t)^{n_2} M(t), \quad \frac{dm(t)}{dt} = -2(k_+ m(t) - k_{off})P(t) \quad , \tag{1}$$

where P(t) is the fibril number concentration, M(t) is the fibril mass concentration, m(t) is the monomer concentration, k_n is the primary nucleation rate constant, k_2 is the secondary nucleation rate constant, and k_+ and k_{off} are the rate constants for fibril elongation and monomer dissociation.

An accurate solution for the monomer mass can be constructed as (2, 3):

$$\frac{m(t)}{m_{tot}} = (1-\varepsilon)\frac{\kappa^2}{\lambda^2 \cosh(\kappa t) + \kappa^2 - \lambda^2} + \varepsilon, \tag{2}$$

where $\lambda = \sqrt{2k_+ k_n {m_{tot}}^{n_c}}$, $\kappa = \sqrt{2k_+ k_2 {m_{tot}}^{n_2+1}}$, and $\varepsilon = k_{off}/(k_+ m_{eq})$. Similarly, a formula for P(t) can be constructed as (4):

$$P(t) = P(\infty)\left[1 - \left(\frac{m(t)}{m_{tot}}\right)^{\frac{1}{\theta}}\right] + k_2 {m_{tot}}^{n_2} \varepsilon^{n_2}(1-\varepsilon)t, \tag{3}$$

where $\theta = \sqrt{2/[n_2(n_2+1)]}$ and $P(\infty) = \kappa\theta/(2k_+)$. Finally, combining Eqs. (2) and (3), we obtain an expression for the average length as:

$$\langle j \rangle = \frac{m_{tot} - m(t)}{P(t)}. \tag{4}$$

The performance of the analytical solutions (2), (3) and (4) against numerical integration of Eq. (1) is demonstrated in Fig S5. In particular, Eq. (4) shows that the average length of aggregates evolves through two main timescales (see Fig S5d). Initially, monomer dissociation is negligible compared to elongation and the aggregation reaction proceeds in the forward direction leading to an increase of fibril lengths. After the monomer concentration has equilibrated, dissociation becomes important and the system enters a slow length redistribution phase where the average length decreases with time and the system eventually reaches equilibrium. Note that since free monomers are no longer available in this second regime, small filaments break up to release new monomers that are incorporated by the longer aggregates, in analogy to Ostwald ripening.

The data of average length (Figure 1b-ii in the main text) were fitted to equation (4) assuming $n_2 = n_c = 2$. Moreover, the depolymerisation rate k_{off} was expressed in terms of the elongation rate, k_+, and the equilibrium free monomer concentration, m_{eq}, as $k_{off} = k_+ m_{eq}$. The equilibrium free monomer concentration was estimated to be lower than 0.5 μM by SDS-PAGE analysis (see supporting Figure 2).

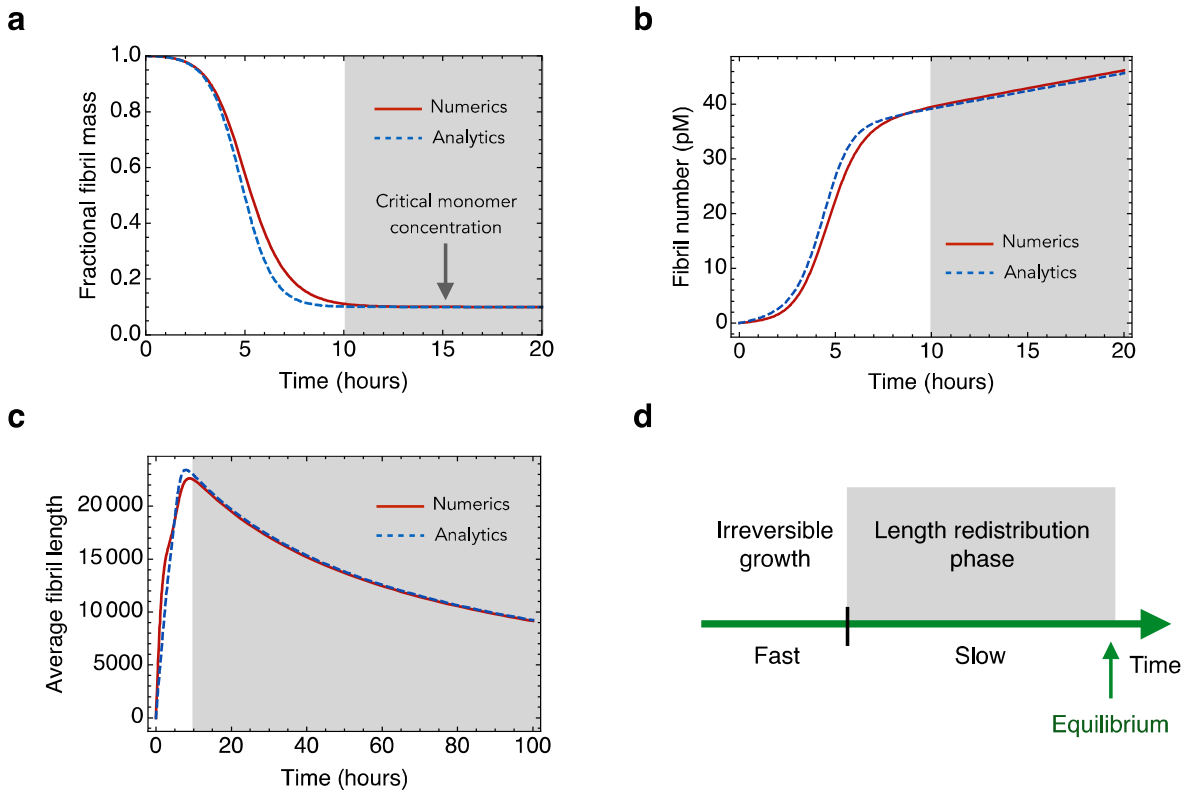

Supporting Figure 5 Accuracy of analytical solutions for secondary nucleation and ripening model and summary of timescales involved in the problem

a)-c) Comparison between numerical solution of Eq. (1) and the analytical solutions Eqs. (2), (3) and (4) for fibril mass concentration (a), fibril number concentration (b) and average fibril length (c), respectively. The calculation parameters are: $m_{tot} = 1\mu M$, $k_n = 10^{-4}M^{-1}s^{-1}$, $k_2 = 2 \times 10^4 M^{-2}s^{-1}$, $k_+ = 3 \times 10^6 M^{-1}s^{-1}$, $m_{eq} = 0.1\ \mu M$, $n_2 = n_c = 2$.
d) Schematic representation of the timescales involved in reversible polymerization: initially aggregates grow irreversibly and the average length increases; after monomers equilibrate, the system enters a slow length redistribution phase where the average length slowly decreases with time and the system approaches equilibrium (ripening phase).

References

1. Sang JC, et al. Direct observation of protein aggregate replication in vitro to model prion and prion-like diseases.

2. Michaels TCT, Garcia GA, Knowles TPJ (2014) Asymptotic solutions of the Oosawa model for the length distribution of biofilaments. *J Chem Phys* 140(19):194906.

3. Michaels TCT, Lazell HW, Arosio P, Knowles TPJ (2015) Dynamics of protein aggregation and oligomer formation governed by secondary nucleation. *J Chem Phys* 143(5):054901.

4. Michaels TCT, Cohen SIA, Vendruscolo M, Dobson CM, Knowles TPJ (2016) Hamiltonian Dynamics of Protein Filament Formation. *Phys Rev Lett* 116(3):038101.